Caveolin-1–Deficient Mice Have Increased Tumor Microvascular Permeability, Angiogenesis, and Growth

Michelle I. Lin, Jun Yu, Takahisa Murata, and William C. Sessa

Department of Pharmacology, Boyer Center for Molecular Medicine, Yale University, New Haven, Connecticut

Abstract

Caveolin-1 (Cav-1) is a major structural protein that is essential to the formation of the organelle, caveolae. Cav-1 knockout (KO) mice were observed to be completely devoid of caveolae yet they exhibit a hyperpermeable vasculature. Given the nature of the hyperpermeable Cav-1 KO endothelium, we sought to investigate if tumors grown in Cav-1 KO mice would be leaky and grow faster. Indeed, Lewis lung carcinoma cells implanted into Cav-1 KO mice had increased tumor vascular permeability, measured by Evans blue extravasation and fibrinogen deposition compared with tumors implanted into wild-type (WT) mice. Cav-1 KO mice also had significantly higher tumor growth rates, attributable to increased tumor angiogenesis and decreased tumor cell death. Furthermore, administration of an antipermeability peptide, cavtratin, was able to correct the tumor hyperpermeability as well as attenuate the increased tumor growth. Mechanistically, endothelial cells isolated from Cav-1 KO mice exhibited increased tyrosine phosphorylation on vascular endothelial growth factor (VEGF) receptor-2 (VEGFR-2) and decreased association with the adherens junction protein, VE-cadherin. Thus, the loss of Cav-1 increases tumor permeability and growth and that may relate to enhanced VEGF signaling due to lack of Cav-1 inhibition of VEGFR-2 or decreased VE-cadherin mediated VEGFR-2 phosphorylation. [Cancer Res 2007;67(6):2849–56]

Introduction

One consistently observed abnormality of the tumor vasculature is its leakiness to macromolecules (1). As a result, extravasation of plasma or plasma proteins across the microvascular wall into the interstitial space of tumors occurs and this is likely due to ultrastructural abnormalities such as widened interendothelial junctions, discontinuous or even absent basement membrane, and numerous transcellular openings (2). The direct relevance of tumor permeability to tumor progression is not clear; however, the degree of vascular leak increases with the histologic grade and malignant potential of certain tumors (3). One mechanism of how vascular leak contributes to tumor progression is that the leakage of plasma proteins, such as fibrin/fibrinogen, can alter the extracellular matrix generating a provisional stroma that is proangiogenic (4). This, in turn, can influence growth factor availability (via sequestration of growth factors), as well as their synthesis and degradation. Therefore, it is likely that vascular permeability may be an important determinant for the angiogenic potential of tumors.

Recently, there are reports demonstrating that modulation of tumor permeability may regulate tumor progression. For example, angiopoietin-1–overexpressing transgenic mice are resistant to vascular endothelial growth factor (VEGF)–induced vascular leakage (5, 6) and human colon cancer cells (HT29)–overexpressing angiopoietin-1 can significantly reduce VEGF-mediated increases in vascular permeability and grow slower when implanted into mice (7). In a different model, treatment of mice bearing tumors with an antipermeability peptide, called cavtratin, acutely reduces tumor microvascular permeability and subsequently attenuates tumor progression in mice (8). Furthermore, the angiogenesis inhibitors angiostatin and TNP-470 also acutely reduce vascular leakage in two models of retinopathy (9) as well as VEGF-mediated vascular permeability in mouse skin and tumors (10). These antiangiogenic agents, although effective in targeting endothelial angiogenic properties such as proliferation and migration resulting in reduced tumor growth, all have significant effects in reducing tumor permeability, suggesting that the concept of antiangiogenic therapy could probably extend beyond blocking strictly angiogenesis but also vascular permeability as well.

Vascular permeability can occur either through a transcellular route or paracellular pathways and one potential transcellular pathway may occur via caveolae. Caveolae can constitute up to 30% of endothelial surface area in capillaries and provide a means of transcellular transport of macromolecules (11). Interestingly, in mice deficient in the gene for caveolin-1 (Cav-1), the main structural coat protein for caveolae in endothelial cells, epithelial cells, adipocytes, smooth muscle, and fibroblasts, radio-iodinated albumin is cleared from circulation at an accelerated rate and these mice exhibit a striking hyperpermeable phenotype in their vasculature (12). Because Cav-1 is a negative regulator of nitric oxide (NO) synthesis, it was proposed that the increase in permeability is a NO-dependent process because administration of *N*-nitro-L-arginine methyl ester (L-NAME), a well-established inhibitor of NO synthase, rescued the hyperpermeable phenotype seen in Cav-1 knockout (KO) mice (12). One hypothesis that derived from these observation was that because Cav-1 was an endogenous inhibitor of endothelial NO synthase (eNOS), the loss of Cav-1 may result in hyperactivation of eNOS and that NO may play a role in altering blood flow and paracellular junctional permeability.

In light of the hyperpermeable characteristics of the Cav-1 KO vasculature, we sought to test our hypothesis that permeability contributes to tumor progression. Thus, the goal of our present study was to examine whether the hyperpermeability observed in Cav-1 KO mice vasculature can also be extended to the tumor vasculature and whether this contributes to an increase in tumor progression.

Note: Current address for T. Murata: Department of Veterinary Pharmacology, Graduate School of Agriculture and Life Sciences, University of Tokyo, Tokyo 113-8657, Japan.

Requests for reprints: William C. Sessa, Vascular Biology and Transplantation Program, Department of Pharmacology, Boyer Center for Molecular Medicine, Yale University School of Medicine, New Haven, CT 06536. Phone: 203-737-2213; Fax: 203-737-2290; E-mail: william.sessa@yale.edu.

©2007 American Association for Cancer Research.

doi:10.1158/0008-5472.CAN-06-4082

Downloaded from http://aacrjournals.org/cancerres/article-pdf/67/6/2849/2580578/2849.pdf by guest on 06 November 2024

Materials and Methods

Animals. Mice were housed and maintained in the local facility, and all experiments were approved by the institutional animal care and use committees of Yale University. Cav-1 KO mice (13) and their respective control wild-type (WT) mice of the same generation were bred and used between 6 and 8 weeks of age. Genotypes of WT and Cav-1 KO mice were confirmed by PCR using the forward primer 5′-TTTACCGCTTGTTGTC-TACGA-3′ and reverse primer 5′-TATCTCTTTCTGCGTGCTGA-3′, and forward primer 5′-TATTCTGCCTTCCTGATGATAACTG-3′ and reverse primer 5′-CCTGCGTGCAATCCATCTTGTTCAATG-3′, respectively.

Mouse endothelial cell isolation and culture. Mouse lung endothelial cells (MLEC) were isolated from WT or Cav-1 KO mice as previously described (14). After immortalization with polyoma middle T-antigen (a gift from Drs. Luca Primo and Federico Bussolino), immunoisolated endothelial cells were culture in EBM-2/EGM-2 MV medium (Cambrex, East Rutherford, NJ).

Tumor implantation. Lewis lung carcinoma (LLC) cells (10^6) were injected s.c. in the back of 6- to 8-week-old WT or Cav-1 KO mice. When tumors became palpable, they were monitored for tumor growth by measuring the length and width of the tumor using a caliper, and tumor volume was determined by the following formula: volume = $0.52 \times (\text{width})^2 \times (\text{length})$. For experiments with peptide, mice were randomly separated into different treatment groups and injected i.p. with 2.5 mg/kg of antennapedia or cavtratin (8) peptides daily. Cavtratin peptide is a fusion peptide composed of the putative scaffolding domain of Cav-1 (amino acids 82–101; DGIWKASFTTFTVTKYWFYR) and the antennapedia internalization sequence (RQIKIWFQNRRMKWKK; ref. 8).

Tumor permeability. Mice with implanted tumors between 1,000 and 2,500 mm^3 were either untreated or injected with antennapedia or cavtratin (2.5 mg/kg; i.p) at 16 and 1 h before being anesthetized so that Evans blue can be administered for 30 min (30 mg/kg i.v.). Subsequently, mice were sacrificed and perfused with PBS through the left ventricle to clear the dye from the vascular volume. Tumor masses were excised, dried in 60°C overnight, and weighed before Evans blue extraction using formamide at 55°C for 16 h. Evans blue content was quantified by reading at 630 nm in a spectrophotometer.

Immunohistochemistry. Implanted tumors after 7 days or end point tumors were excised and fixed in 3% paraformaldehyde for 2 h before either dehydration using 70% ethanol and processed for paraffin embedding or dehydration using 30% sucrose/PBS and frozen in compound. To visualize the amount of fibrinogen deposition around tumor blood vessels, 5 μm frozen sections of tumor tissue were permeabilized and blocked with 0.1% Triton X-100, 0.2% bovine serum albumin, and 5% normal donkey serum in PBS. Tissue sections were then incubated with α-fibrinogen (DAKO, Carpinteria, CA) and α–platelet/endothelial cell adhesion molecule 1 (PECAM-1; PharMingen, San Jose, CA) before incubation with Alexa 488– and Alexa 594–conjugated secondary antibodies (Molecular Probes, Carlsbad, CA) and coverslipping with 4′,6-diamidino-2-phenylindole (DAPI) containing mounting medium. To quantify the amount of colocalization between fibrinogen and PECAM-1, between three and six areas per slide were scored from five or six tumors from Cav-1 KO or WT mice, respectively. Each area was quantified using the colocalization module in Openlab software (Improvision, Lexington, MA), and areas of colocalization were normalized to the amount of PECAM-1–positive pixel density.

To quantify tumor vasculature, 60 μm frozen sections of 7-day tumor tissue were permeabilized and blocked using 0.3% Triton X-100 and 5% normal goat serum in PBS for 1 h. Tissue sections were then incubated with α-PECAM-1 or α-VE-cadherin (PharMingen) in blocking solution for 16 h at room temperature before Alexa 488–conjugated secondary antibody incubation in blocking solution for 6 h. Fluorescent images were captured using a Zeiss microscope and analyzed using the Openlab image analysis software. At least two areas per tumor were analyzed, and images of each area were captured over the range of 40- to 44-μm-thick, compiled as a Z-series of 2-μm-thick slices. Each Z-series slice was subtracted for background, and 19 slices deconvolved to minimize overlapping fluorescence from adjacent slices. The final image was derived from a composite of 19 processed slices and used for pixel density quantitation by the Openlab software to generate the percentage of positive areas relative to the total observed tumor area.

To label proliferative nuclei, 5-μm paraffin sections from 7- or 12-day tumor tissues were immunostained for Ki-67. The number of Ki-67–positive nuclei were manually counted from four random nonnecrotic areas per tissue sections (two sections per tumor) and normalized to the total number of hematoxylin-stained nuclei (between 500 to 1,500 nuclei scored per area).

Terminal deoxyribonucleotide transferase–mediated nick-end labeling assay. Paraffin-embedded tumor tissue sections were processed for terminal deoxyribonucleotide transferase–mediated nick-end labeling (TUNEL)–positive nuclear staining using ApoTag kit (Chemicon, Temecula, CA) similar to previously described (8). At least five to eight random nonnecrotic areas of the tumor sections from two sections of each tumor mass were quantified for TUNEL-positive nuclei using Scion Image 1.62 and normalized to total area quantified.

VEGF ELISA. Flash-frozen tumor tissue from end point tumors were pulverized on dry ice and homogenized using a rotor-stator homogenizer (PowerGen 125, Fisher Scientific, Pittsburgh, PA) to allow efficient lysis in modified radioimmunoprecipitation assay buffer (RIPA) containing 50 mmol/L Tris-HCl (pH 7.4), 0.1 mmol/L EGTA, 0.1 mmol/L EDTA, 1% NP40, 0.1% SDS, 0.1% DOC, 1 mmol/L sodium orthovanadate, 20 mmol/L NaF, 1 mmol/L $Na_4P_2O_7$, 1 mmol/L Pefabloc SC, and protease inhibitor cocktail (Roche Diagnostics, Indianapolis, IN). After normalizing for total protein concentration, tumor samples were used to determine VEGF levels in the tumors by ELISA (Quantikine mouse VEGF Immunoassay, R&D Systems, Minneapolis, MN).

Immunoprecipitation and Western blotting. MLECs were serum starved in EBM-2 medium for 36 to 48 h before stimulating with VEGF (100 ng/mL) for the indicated times. Cells were rinsed with ice-cold PBS and lysed in modified RIPA lysis buffer and subjected to immunoprecipitation with VEGFR-2 antibody (Santa Cruz Biotechnology, Santa Cruz, CA) and/or Western blotting with phosphotyrosine (pTyr, 4G10, Upstate), VE-cadherin (PharMingen), Cav-1 (Santa Cruz Biotechnology), Hsp90, and Cav-2 (Transduction Laboratories, Lexington, KY) similar to previously described (8).

Results

Tumors implanted into Cav-1 KO mice have increased microvascular permeability and growth. Previous studies have shown that the loss of Cav-1 increased vascular permeability in various vascular beds (12). To address whether the loss of host Cav-1 also affected tumor vascular permeability, LLC cells were implanted onto backs of 6- to 8-week-old WT and Cav-1 KO mice. When tumor sizes reached between 1,000 and 2,500 mm^3, Evans blue was injected, mice were perfused with PBS, dye was subsequently extracted, and samples were quantified spectrophotometrically. Figure 1*A* shows that Cav-1 KO mice had significantly higher Evans blue extravasation than WT mice. Quantitative measurements of tumor hyperpermeability have generally been made using macromolecular tracers such as fibrin/fibrinogen (15). Its insoluble nature does not allow it to re-enter the blood or lymphatic circulation without proteolytic degradation; thus, fibrin/fibrinogen deposition has also been used as surrogate measurement for tumor blood vessel permeability (16). We examined the amount of fibrinogen deposition in tumor tissue sections by double labeling of fibrinogen and PECAM-1. Figure 1*B* is a representative figure of tumor fibrinogen shown by red fluorescence (Alexa 594) with the amount of PECAM-1–positive blood vessels indicated by green fluorescence (Alexa 488) from WT and Cav-1 KO mice. As shown, there is more fibrinogen staining around the tumor microvasculature in the Cav-1 KO than WT mice and after normalizing to total area of vascular density (WT 5.9% and KO 8.3%), tumors in Cav-1 KO had increased fibrinogen colocalization

Downloaded from http://aacrjournals.org/cancerres/article-pdf/67/6/2849/2580578/2849.pdf by guest on 06 November 2024

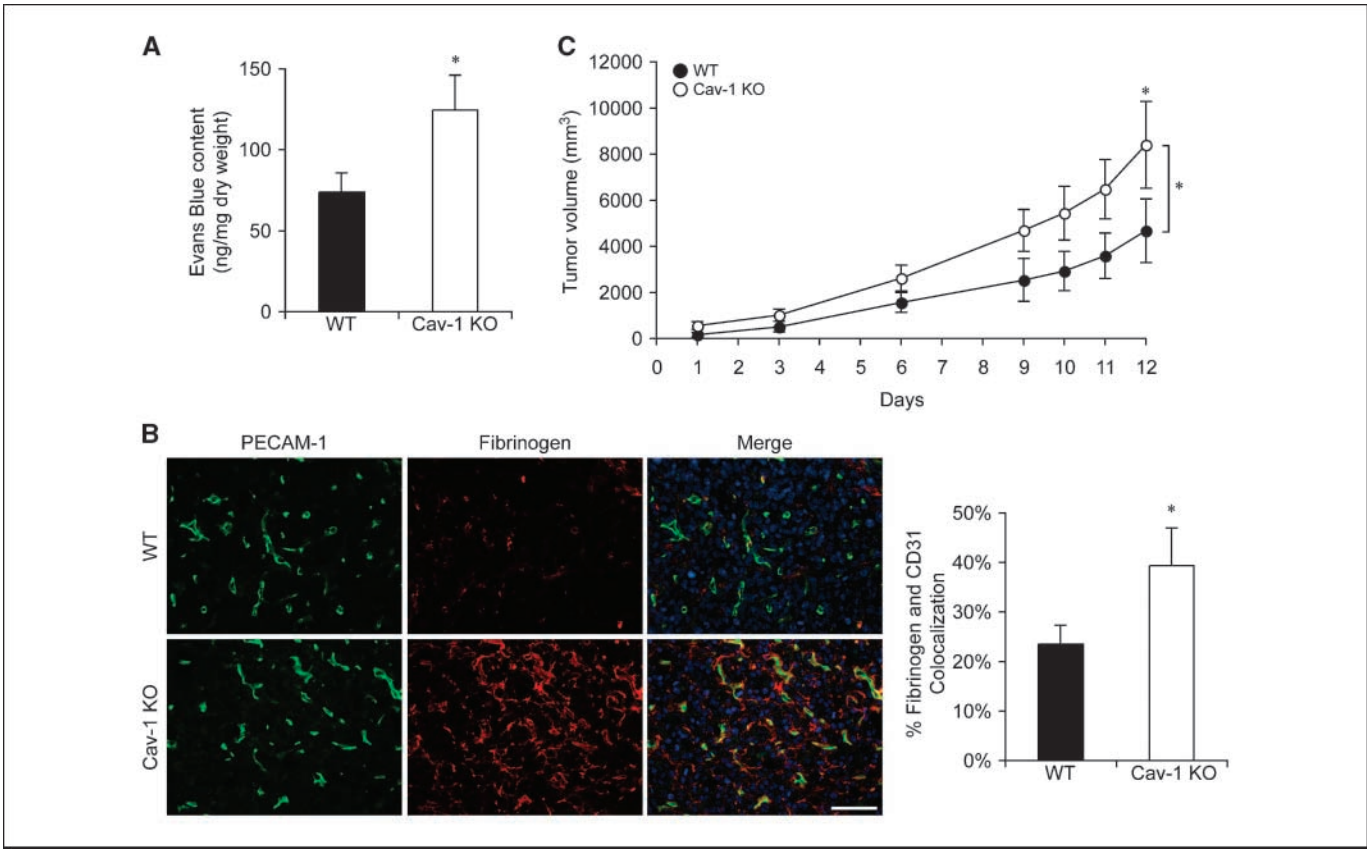

Figure 1. Tumors implanted into Cav KO mice have increased tumor microvascular permeability and growth. *A,* 10^6 LLC cells were implanted s.c. in the lower back of 6- to 8-wk-old male WT or KO mice. Mice with tumor sizes between 1,000 and 2,500 mm^3 were used to measure vascular permeability by Evans blue extravasation (30 mg/kg, i.v.; 30 min) as an index of albumin leakage. Evans blue was extracted in formamide at 55°C for 24 h and quantified spectrophotometrically at 630 nm. Note the increase in tumor microvascular permeability in Cav KO mice. *, $P < 0.05$, compared with Cav WT by Student's *t* test ($n = 12$ for WT and $n = 16$ for KO). *B,* to characterize the hyperpermeable phenotype of tumors implanted into Cav-1 KO mice, LLC implanted s.c. in WT or KO mice were excised at day 14 (end point tumor) and fixed in 3% paraformaldehyde. Frozen sections (5 μm) of the tumor tissue were double immunofluorescently labeled for blood vessels (PECAM-1, *green*) and fibrinogen (*red*). The sections were counterstained with DAPI for nuclear labeling (*blue*). The percentage of fibrinogen and PECAM-1 colocalization (*yellow*) was quantified and normalized to total PECAM-1–positive pixel density. *Columns,* mean; *bars,* SE. *, $P < 0.05$ compared with WT by Student's *t* test ($n = 6$ for WT and $n = 5$ for KO). *C,* to monitor the effect of hyperpermeability on tumor progression, LLC cells were implanted in WT or KO mice similar to those in (*A*) and when tumors become palpable, tumor size was monitored every 2 d using a caliper and allowed to progress for 12 d. Tumors implanted in the Cav-1 (−/−) mice exhibited increased tumor progression. *, $P < 0.001$, compared with WT by two-way ANOVA ($n = 5$ for WT and $n = 8$ for KO); *, $P < 0.05$ using Bonferroni post hoc test at day 12. Representative of two separate experiments. *Bar,* 100 μm.

with PECAM-1–positive blood vessels (Fig. 1*B, inset*). Thus, tumors implanted into Cav-1 KO mice exhibit increased accumulation of Evans blue and fibrinogen consistent with enhanced microvascular leakage in these mice. To examine if increased tumor permeability affected the growth of the tumors, the growth of LLC implanted into both WT and Cav-1 KO mice was monitored over time. As seen in Fig. 1*C*, LLC implanted into Cav-1 KO mice grew faster than LLC in WT mice (Fig. 1*C*). This experiment was repeated twice with similar results. Thus, these data support the hypothesis that increased tumor microvascular permeability can contribute to increased tumor growth.

LLC tumors implanted in Cav-1 KO mice have increased angiogenesis. To assess tumor angiogenesis, tumors were labeled using antibodies to the endothelial specific markers, VE-cadherin or PECAM-1. An early time point was chosen for this study, as end point tumor masses tend to exhibit large areas of necrosis and more heterogeneous patterns of tumor vasculature. Also, to better visualize the complexity and depth of the tumor vasculature, thick tumor sections (60 μm cryosections) were used. As seen in Fig. 2*A*, in the representative deconvolved images of the tumor sections stained for VE-cadherin, the vasculature in tumors found in Cav-1 KO mice was more compact with greater branch points and density. Quantification of VE-cadherin–positive areas relative to total areas examined show that tumor angiogenesis was greater in tumors implanted into Cav-1 KO mice compared with WT mice (Fig. 2*A, right*). These data suggest that tumors implanted into a host environment that is deficient in Cav-1 promoted angiogenesis.

Tumors implanted in the Cav-1 KO mice had decreased apoptosis with no change in tumor cell proliferation. Another possible mechanism that may explain the increase in tumor size in Cav-1 KO mice is whether tumors exhibit decreased cell death or increased proliferation. To assess the amount of tumor apoptosis, TUNEL-positive cells in tumor sections after 7 days of growth in WT and Cav-1 KO mice were examined. As the TUNEL assay will also label necrotic cells, we carefully counted the number of apoptotic nuclei in at least five to eight random nonnecrotic areas of the tumors per animal and quantified per area using Scion Image analysis software. The analysis revealed that Cav-1 KO mice exhibited significantly decreased tumor cell apoptosis (Fig. 2*B*). Next, we examined the extent of tumor cell proliferation using an antibody to Ki-67 antigen to label proliferating cells in early (7 days) and end point (12 days) tumor tissues from WT and Cav-1

Downloaded from http://aacrjournals.org/cancerres/article-pdf/67/6/2849/2580578/2849.pdf by guest on 06 November 2024

KO mice. After normalizing for the total number of nuclei counted, there was no significant difference in the proliferative index between WT and Cav-1 KO mice at either of the time points examined (Fig. 2*C*). We also quantified the amount of VEGF ($VEGF_{120}$ and $VEGF_{164}$) in tumors by ELISA. Figure 2*D* shows that there were significantly lower levels of VEGF found in LLC tumors implanted in the Cav-1 KO mice. Together, these data show that tumors implanted in the Cav-1 KO mice were larger, due to increased angiogenesis, and enhanced tumor cell survival without a change in proliferative index or VEGF levels.

Cavtratin significantly decreases tumor hyperpermeability in Cav-1 KO mice and results in attenuated tumor growth. Previously, we have shown that cavtratin, a cell-permeable peptide derived from Cav-1 that inhibits eNOS acutely, reduces tumor hyperpermeability, and chronic treatment with this peptide can significantly reduce tumor growth (8). Furthermore, because it has been reported that the hyperpermeability observed in Cav-1 KO mice is due to hyperactivation of eNOS (12, 13), we sought to examine whether cavtratin can also reduce tumor permeability in Cav-1 KO mice by virtue of its ability to inhibit eNOS and serve as a surrogate for endogenous Cav-1. After implanted LLC reached between 1,000 and 2,000 mm^3 in size, mice were randomly separated into two groups for treatment with either the control internalization antennapedia peptide or cavtratin and challenged with Evans blue. As seen in Fig. 1*A*, Cav-1 KO tumors (Fig. 3*A, open columns*) had significantly higher microvascular permeability than those implanted in WT mice (Fig. 3*A, solid columns*) among the control antennapedia peptide groups. Short-term treatment with the cavtratin in WT mice reduced tumor permeability (17). Interestingly, cavtratin administration to the Cav-1 KO mice also significantly decreased tumor microvascular permeability to a similar extent as those observed in WT (Fig. 3*A*). These results indicate that acute administration of an antipermeability agent by virtue of inhibiting eNOS can reduce tumor vascular permeability in a model of elevated tumor vascular permeability.

To further test our hypothesis that chronic intervention at the level of vascular permeability can significantly alter the progression of tumor growth, LLC cells were implanted into WT and Cav-1 KO mice, and mice were randomly separated into two groups, one receiving antennapedia and the other receiving cavtratin. As previously observed in Fig. 1*C*, tumor growth in the control antennapedia-treated Cav-1 KO (○) was significantly faster than that seen in the antennapedia-treated WT (●, Fig. 3*B*). Furthermore, daily treatment of WT mice with cavtratin reduces tumor growth (■ compared with ●, Fig. 3*B*); however, cavtratin markedly reduces tumor growth in LLC implanted into Cav-1 KO mice. Thus, treatment of Cav-1 KO mice with cavtratin decreases tumor

Downloaded from http://aacrjournals.org/cancerres/article-pdf/67/6/2849/2580578/2849.pdf by guest on 06 November 2024

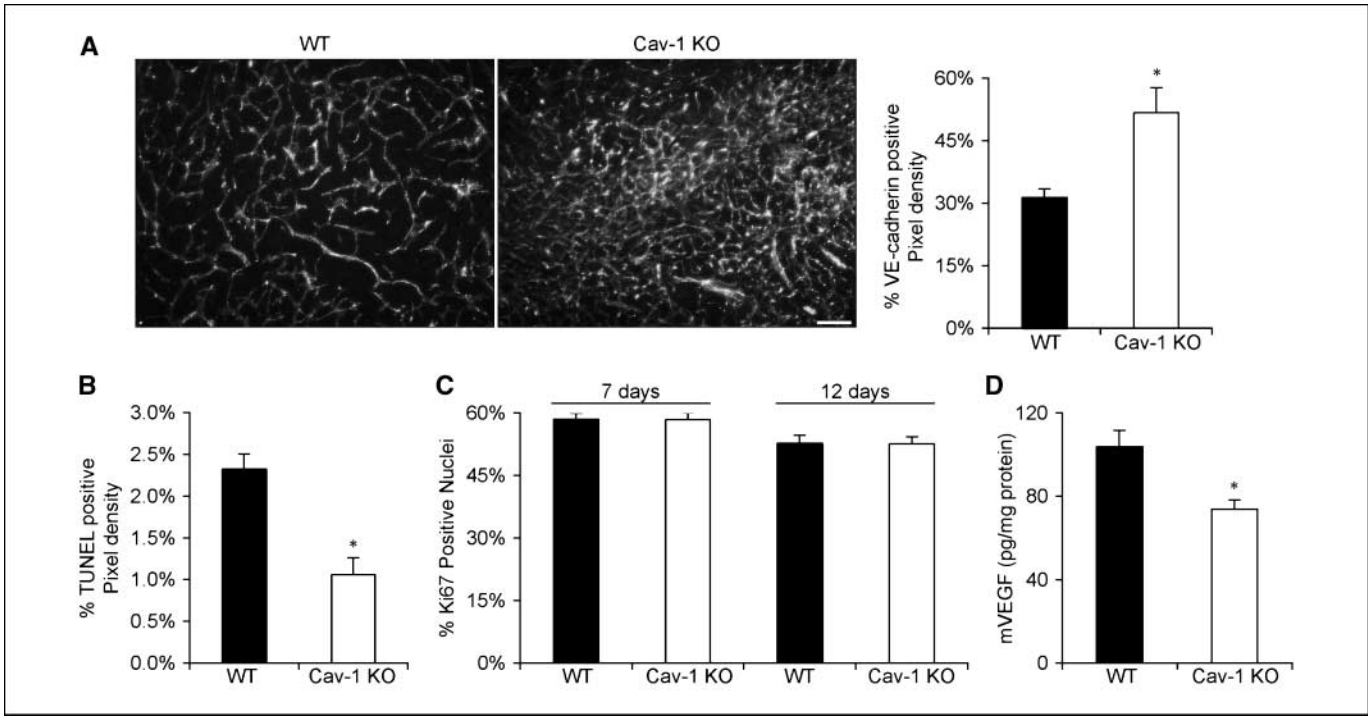

Figure 2. Tumors implanted into Cav-1 KO mice exhibited increased vascularity and decreased apoptosis without changing tumor cell proliferation. *A,* LLC cells implanted s.c. in WT or KO mice were excised at day 7 after tumors become palpable and fixed in 3% paraformaldehyde. Frozen sections (60 μm) of the tumor tissue were immunofluorescently labeled for blood vessels (VE-cadherin, *white*). Immunofluorescent images were captured at 2-μm sections spanning a total of 40 μm per tumor area (two areas per tumor, $n = 4–5$ tumors each); each image was subtracted for background fluorescence and deconvolved using the Openlab software (Improvision). A final merge of 19 sections resulting in a 38-μm-thick section was quantified for the amount of VE-cadherin staining relative to total pixel density. *Columns,* mean; *bars,* SE. *, $P < 0.05$ compared with WT by Student's *t* test. *B,* 5-μm paraffin sections of the tumor tissue were processed for TUNEL staining to label apoptotic nuclei. The total number of apoptotic nuclei was scored from five to eight areas per tissue section and two sections per tumor ($n = 4–5$ per group). The average percentage of TUNEL-positive nuclei per area was compiled from each tumor. *Columns,* mean; *bars,* SE. *, $P < 0.01$ compared with WT by Student's *t* test. *C,* 5-μm paraffin sections of the tumor tissue were also immunohistochemically stained for Ki-67 to label proliferative nuclei and counterstained with hematoxylin to label all nuclei. The total number of Ki-67–positive nuclei was scored from four areas per tissue section and two sections per tumor ($n = 4–7$ per group). The average percentage of Ki-67–positive nuclei per total nuclei was compiled from each tumor. *Columns,* mean; *bars,* SE. *D,* tumor tissue was homogenized and resuspended in homogenization buffer and processed for quantitative ELISA determination of murine $VEGF_{120}$ and $VEGF_{164}$ (R&D Systems). Average levels of murine VEGF: *Columns,* mean ($n = 6$ per group); *bars,* SE. *, $P < 0.01$ compared with WT by Student's *t* test. *Bar,* 100 μm.

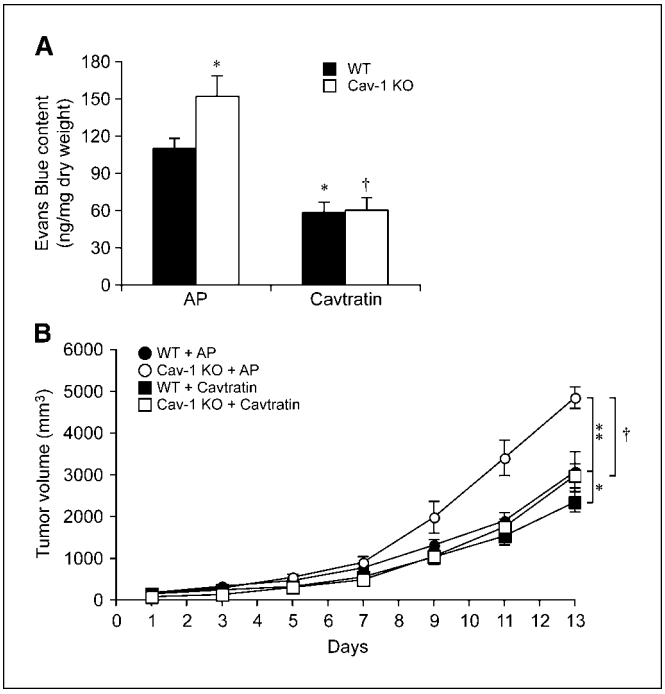

Figure 3. The tumor hyperpermeability and increased tumor growth in Cav-1 KO mice can be decreased by cavtratin. *A,* 10^6 LLC cells were implanted s.c. in WT (■) or Cav-1 KO (□) mice. Mice with tumor sizes between 1,000 and 2,000 mm^3 were randomized to receive either antennapedia (control peptide) or cavtratin at 2.5 mg/kg by i.p. injection at 16 and 1 h before Evans blue injection (30 mg/kg, i.v.; 30 min). Evans blue was then extracted and quantified spectrophotometrically at 630 nm. *, $P < 0.05$, compared with WT mice injected with antennapedia; †, $P < 0.001$, compared with Cav-1 KO mice injected with antennapedia by Student's *t* test ($n = 6$–8 each). *B,* Cav WT (●,■) and KO (○,□) mice were treated with either control antennapedia peptide (●,○) or cavtratin (■,□) at 2.5 mg/kg by i.p. injection daily. Tumor volume measured every 2 d by caliper and plotted. *, $P < 0.005$, compared with WT mice injected with antennapedia ($P < 0.05$ on day 13 by Bonferroni post hoc test); **, $P < 0.0001$ compared with WT mice injected with antennapedia ($P < 0.001$ on days 11 and 13 by Bonferroni post hoc test); †, $P < 0.0001$ compared with Cav-1 KO mice injected with antennapedia ($P < 0.01$ on day 9 and $P < 0.001$ on days 11 and 13 by Bonferroni post hoc test) by two way ANOVA; ($n = 6$ each).

progression to a similar extent as WT mice treated with the control antennapedia peptide.

Cav-1 is important for regulation of VEGFR-2 tyrosine phosphorylation and association with adherens junction complex. To shed light on additional possible mechanisms in which Cav-1 deficiency in the tumor vasculature may contribute to increased tumor angiogenesis and permeability, we isolated endothelial cells from WT and Cav-1 KO mice. Cav-1 was absent in lysates from Cav-1 KO and Cav-2 levels were reduced due to the importance of Cav-1 in stabilizing Cav-2 protein (Fig. 4*A, top*; ref. 18). Because Cav-1 has been shown to associate with and negatively regulate VEGF receptor 2 (VEGFR-2; ref. 19), we examined VEGFR-2 phosphorylation in the absence and presence of VEGF stimulation. As seen in Fig. 4*A* (*bottom*), VEGFR-2 after immunoprecipitation is detected as a doublet (*arrowheads* in Fig. 4*A* and *B*), with the higher molecular weight band representing the highly glycosylated mature form of VEGFR-2 that can be tyrosine phosphorylated (*white arrowhead*) and the lower band representing a presumably less glycosylated form of VEGFR-2 that is not phosphorylated (20–22). In WT endothelial cells, VEGF promotes the time-dependent increase in VEGFR-2 phosphorylation that is maximal at 10 min post stimulation and dissipates by 30 min. In Cav-1 KO endothelial cell, VEGF-stimulated VEGFR-2 tyrosine phosphorylation was more robust and sustained compared with WT endothelial cells (as quantified in Fig. 4*A, right*). Because VEGFR-2 has been previously reported to associate with proteins from the adherens junction such as VE-cadherin and β-catenin (20, 22, 23) that negatively regulate the tyrosine phosphorylation on VEGFR-2 (20), we examined whether the increased tyrosine phosphorylation on VEGFR-2 seen in Cav-1 KO endothelial cells could also be attributed to its lack of association with VE-cadherin. Indeed, we observed decreased basal and VEGF-stimulated association between VEGFR-2 and the VE-cadherin complex in the Cav-1 KO endothelial cells compared with WT endothelial cells (Fig. 4*B, left*, as quantified in *right*). These data suggest that the loss of Cav-1 may enhance VEGFR-2 phosphorylation via reduced association with VE cadherin and, in the context of eNOS hyperactivation, promote vascular permeability and tumor angiogenesis.

Discussion

This article shows that mice deficient in Cav-1 develop more permeable and larger tumors than do normal mice. The hyperpermeable tumors in Cav-1 KO mice (defined by the extravasation of Evans blue and deposition of fibrinogen) are larger due to enhanced angiogenesis and survival of cancer cells. Consistent with the idea that early changes in vascular permeability may contribute to the growth of tumors, treatment of Cav-1 KO mice bearing LLC tumors with cavtratin reduces vascular leakage and tumor growth. These data support the idea that early changes in vascular permeability secondary to angiogenic factors such as VEGF may contribute to tumor growth *in vivo*.

Since the discovery of the caveolae organelle, many studies have tested the importance of caveolae in the regulation of vascular permeability via transcytosis of macromolecules across the endothelium. When Cav-1 KO mice were generated, they were devoid of caveolae in many cell types, because Cav-1 is the major coat protein for the organelle and is necessary for the formation of caveolae (13, 18, 24). With the major transcytotic organelle absent, these mice were predicted to have decreased vascular permeability. Thus, it was rather surprising when Schubert et al. (12) reported enhanced vascular hyperpermeability observed in Cav-1 KO mice. One hypothesis put forth by this report was that because Cav-1 was a tonic inhibitor for eNOS (25), the paradoxical increase in vascular permeability observed in Cav-1 KO mice maybe through a compensatory paracellular pathway via hyperactivation of eNOS as an inhibitor to NOS could partially reverse the hyperpermeability observed in these Cav-1 KO mice (12). eNOS is required for VEGF-driven permeability *in vivo* (8, 26, 27), and eNOS is necessary for tumor microvascular permeability and growth (8, 28). In the present study, tumor permeability was increased in Cav-1 KO mice (Fig. 1*A* and *B*), consistent with the reported increase in albumin clearance from Cav-1 KO circulation (12). Our observations that macromolecule deposition and tumor growth are greater in tumors implanted in Cav-1 KO mice is consistent with the hypothesis that tumor permeability is an important contributing factor supporting tumor growth.

Tumors implanted into the Cav-1 KO mice have increased tumor angiogenesis. This increase in angiogenesis may account for the increased tumor vascular permeability observed in Fig. 1*A*; however, when extravasated fibrinogen was normalized to the tumor vasculature, we still observed increase in permeability by the amount of fibrinogen deposition to the tumor blood vessels (Fig. 1*B, inset*). This suggests that the increased vascular

Downloaded from http://aacrjournals.org/cancerres/article-pdf/67/6/2849/2580578/2849.pdf by guest on 06 November 2024

permeability in the Cav-1 KO mice is an inherent property of the vasculature due to Cav-1 deficiency and contributes to increased angiogenesis (16). Tumor permeability and angiogenesis are most likely interdependent, creating a positive feedback mechanism to support increased tumor growth.

The precise role of Cav-1 in angiogenesis is still far from being elucidated. Both proangiogenic and antiangiogenic effects of Cav-1 have been shown in either Matrigel or tumor models. More specifically, Liu et al. (29) observed in a Matrigel model that overexpression of Cav-1 can enhance endothelial tube formation, implicating a proangiogenic potential of Cav-1. Studies by the same group also showed that B16-F10 tumors implanted in Cav-1 KO had impaired angiogenesis, leading to smaller tumors (30). In contrast to these studies but in agreement with our findings, Brouet et al. (31) reported that Cav-1 overexpression in endothelial cells decreased VEGF-induced migration and prevented endothelial tube formation in Matrigel. Furthermore, cationic lipid-based transfection of Cav-1 increased Cav-1 expression in the tumor vasculature and resulted in decreased tumor growth (31). The apparent discrepancy between the different groups may come from the different models examined. Matrigel models do not mimic a tumor microenvironment where tumor secreted cytokines and growth factors as well as the host inflammatory responses during tumor invasion may influence the angiogenic profile of these tumors. Furthermore, Matrigel models do not take into account permeability aspects of angiogenesis and cavtratin, an antipermeability peptide, while capable of attenuating tumor permeability, angiogenesis, and growth did not influence angiogenesis in Matrigel plugs (8).

To further investigate the effects of Cav-1 deficiency on tumor growth, we examined proliferation and apoptosis in tumors implanted into WT and Cav-1 KO mice. As seen in Fig. 2*B*, tumors implanted into Cav-1 KO mice had decreased apoptosis, whereas their proliferative indices were not augmented (Fig. 2*C*). Studies by Holmgren et al. revealed that tumor cells of dormant metastases remain dormant when the high rate of tumor cell proliferation is balanced by a high rate of tumor cell apoptosis and that antiangiogenic therapy with endostatin (32), angiostatin (33), and TNP-470 (34) shifts this equilibrium to increase cell death without apparent changes in the tumor cell proliferative index (34). Furthermore, Garcia-Barros et al. (35) showed that tumors implanted into mice that are resistant to endothelial cell apoptosis had increased tumor growth and less sensitivity to radiotherapy. These studies indicate that tumor growth is highly dependent on the survival of host endothelial cells and less on the active proliferation of tumor cells. From our studies, we did not delineate the apoptotic and proliferative indices between tumor cells or host endothelial cells. Thus, we cannot rule out the effect of Cav-1 deficiency in promoting endothelial cell survival or proliferation, which ultimately may contribute to the increased angiogenesis seen in the tumor vasculature in Cav-1 KO mice.

Previously, we reported that cavtratin significantly decreased tumor permeability after acute administration (8). This peptide was originally designed as a fusion peptide that couples the cell-permeable peptide, antennapedia, to the caveolin scaffolding domain of Cav-1, the latter capable of binding directly to eNOS and inhibit its catalytic activity (25, 36). Furthermore, this peptide, by virtue of its ability in inhibiting eNOS-mediated vascular permeability (37), also led to significant decrease in tumor growth with chronic administration (8). In the present study, we show that acute administration of cavtratin reversed the hyperpermeable state of the Cav-1 KO tumor microvasculature to a comparable

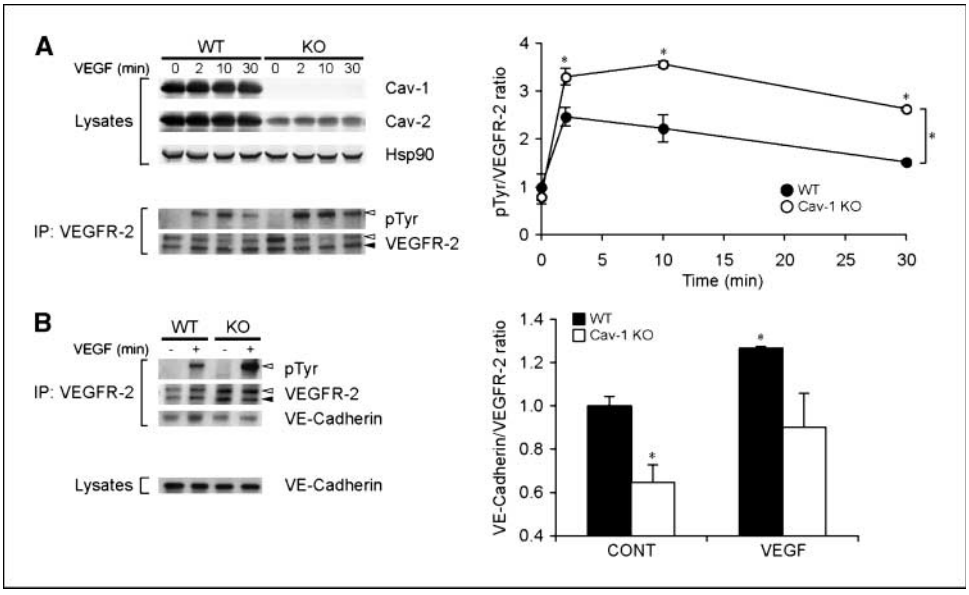

Figure 4. Cav-1 KO MLECs have increased VEGFR-2 phosphorylation and decreased association with the adherens junction complex protein, VE-cadherin. *A,* endothelial cells were isolated from WT and Cav-1 KO mice and plated until confluency before stimulating with VEGF (100 ng/mL) for the indicated times. Lysates were Western blotted for total amounts of Hsp90 (as loading control), Cav-1, and Cav-2. The absence of Cav-1 with concomitant decreased Cav-2 expression confirmed the genotype. Cell lysates were then immunoprecipitated for VEGFR-2 and Western blotted for tyrosine phosphorylated VEGFR-2 (pTyr) and total VEGFR-2. VEGFR-2 is present in two forms (*arrowheads*) with the higher glycosylated form (*white arrowhead*) being one that is tyrosine phosphorylated. Note the hyperphosphorylation of VEGFR-2 in response to VEGF in the Cav-1 KO endothelial cells. These blots are representative of three different experiments. *Points,* relative mean densitometric ratios of pTyr to VEGFR-2; *bars,* SE. *, $P < 0.0001$, compared with WT by two-way ANOVA (*, $P < 0.01$ at times 2, 10, and 30 by Bonferroni post hoc test). *B,* similar to (*A*), the adherens junction protein, VE-cadherin was coimmunoprecipitated with VEGFR-2 before and after VEGF stimulation. There is less association between VEGFR-2 and VE-cadherin in Cav-1–deficient endothelial cells. *Columns,* relative mean densitometric ratios of VE-cadherin to total levels of VEGFR-2 were plotted from three different experiments; *bars,* SE. *, $P < 0.05$ compared with WT CONT.

Downloaded from http://aacrjournals.org/cancerres/article-pdf/67/6/2849/2580578/2849.pdf by guest on 06 November 2024

level seen in WT (Fig. 3*A*). Furthermore, this peptide can significantly decrease tumor progression in Cav-1 KO mice to a similar growth rate as WT mice (Fig. 3*B*). These data are in accordance with a previous report where Schubert et al. (12) reported that administration of a NOS inhibitor, L-NAME, could reduce the hyperpermeability phenotype observed in the Cav-1 KO mice. Thus, the significant effect of this peptide in Cav-1 KO seen here implies that the hyperpermeability mediated by Cav-1 deficiency is, in part, due to eNOS hyperactivation [also reported by Drab et al. (13), who observed increased cyclic guanosine 3′,5′-monophosphate accumulation in Cav-1 KO tissues]. Together, these studies corroborate the importance of eNOS in mediating tumor permeability and ultimately tumor angiogenesis and growth.

In an attempt to address other potential mechanisms in which Cav-1 deficiency can contribute to increased permeability, we first determined whether the increase in angiogenesis and permeability seen in tumors implanted in Cav-1 KO mice was due to increased local production of VEGF using the ELISA-based assay. VEGF is overexpressed in most tumors; in fact, expression levels of VEGF correlates often with malignant progression. The unexpected finding that Cav-1 KO mice had tumors with decreased levels of VEGF (Fig. 2*D*) show that the hyperpermeability in these tumors maybe due to increased VEGFRs expressed on tumor vasculature, and, thus, less VEGF is required to elicit an angiogenic response. In addition, there may be VEGF-independent pathways that contribute to the hyperpermeability state and increased growth rate (38).

On the other hand, the decreased levels of VEGF observed in tumors from Cav-1 KO mice may also be speculated as a result of altered tumor hypoxic microenvironment because we observed an increase in vascular density in these tumors (Fig. 2*A*). Without examining the degree of oxygenation in these tumors, we cannot rule out the effect of hypoxia and, thus, more studies are needed to delineate the causal relationship between vascular density, permeability, and VEGF expression in tumors implanted in WT and Cav-1 KO mice.

To further examine the mechanisms in which Cav-1 deficiency contributes to an increased angiogenic response, we isolated endothelial cells from WT and Cav-1 KO mice. We observed that VEGFR-2 is hyperphosphorylated in Cav-1 KO endothelial cells in response to VEGF compared with WT endothelial cells (Fig. 4*A*). Interestingly, Cav-1 has been previously found to negatively regulate VEGFR-2 activation (19) and *in vitro* incubation of endothelial cell lysates with the scaffolding domain of Cav-1 fused to glutathione *S*-transferase (GST-Cav$_{61\text{-}101}$) decreased VEGFR-2 autophosphorylation (19). Akin to the inhibitory effect of Cav-1 on eNOS, it is feasible that removal of Cav-1 relieves the inhibitory actions on VEGFR-2 and allows for hyperphosphorylation in response to VEGF. This may also explain why we observed increased tumor permeability and angiogenesis in Cav-1 KO mice despite decreased levels of tumor-secreted VEGF (Fig. 2*D*).

The hyperpermeability of tumor vasculature in Cav-1 KO mice (Fig. 1*A* and *B*) prompted us to investigate whether VE-cadherin, a key modulator of paracellular permeability, played a role in regulating permeability in the absence of Cav-1 because VE cadherin interacts with VEGFR-2 (20, 22, 23, 39) and regulates the dephosphorylation of VEGFR-2. In Cav-1 KO endothelial cells, immunoprecipitation of VEGFR-2 resulted in a reduced basal and VEGF-stimulated interaction with VE-cadherin and β-catenin (Fig. 4*B* and data not shown) that correlated with increased VEGFR-2 phosphorylation. Our observation that Cav-1 is important for VEGFR-2 and VE-cadherin interactions adds another level of complexity to the role of VE-cadherin in regulating VEGF signaling and suggests that Cav-1 may serve as a docking partner for the regulation of VEGFR-2 by VE-cadherin and other associated kinases/phosphatases.

In conclusion, we have provided evidence that Cav-1 is an important mediator of tumor vascular permeability such that genetic ablation of host Cav-1 results in a hyperpermeable endothelium, allowing macromolecules to extravasate into the tumor interstitium. The hyperpermeability observed contributes to increased tumor growth and angiogenesis, promoting tumor cell survival. Mechanistically, Cav-1–mediated increase in permeability is in part due to changes in the modulation of VEGFR-2 phosphorylation and interaction with adherens junction proteins. The negative effect of Cav-1 on VEGFR-2 phosphorylation and eNOS may additively contribute to the increased tumor permeability, survival and ultimately tumor growth.

Acknowledgments

Received 11/6/2006; revised 12/22/2006; accepted 1/17/2007.

Grant support: NIH grants R01 HL64793, RO1 HL 61371, R01 HL 57665, and PO1 HL 70295 (W.C. Sessa).

The costs of publication of this article were defrayed in part by the payment of page charges. This article must therefore be hereby marked *advertisement* in accordance with 18 U.S.C. Section 1734 solely to indicate this fact.

We thank Drs. Marek Drab and Teymuras Kurzchalia (Max Planck Institute, Dresden, Germany) for the Cav-1 KO mice; Dr. Donald McDonald (Department of Anatomy, University of California San Francisco, San Francisco, CA) for providing the protocol for thick tissue section immunofluorescent labeling; and Drs. Luca Primo and Federico Bussolino (University of Torino, Turin, Italy) for providing the polyoma middle T-antigen retrovirus for MLEC immortalization.

Downloaded from http://aacrjournals.org/cancerres/article-pdf/67/6/2849/2580578/2849.pdf by guest on 06 November 2024

References

1. Dvorak HF, Nagy JA, Dvorak JT, Dvorak AM. Identification and characterization of the blood vessels of solid tumors that are leaky to circulating macromolecules. Am J Pathol 1988;133:95–109.
2. Hashizume H, Baluk P, Morikawa S, et al. Openings between defective endothelial cells explain tumor vessel leakiness. Am J Pathol 2000;156:1363–80.
3. Daldrup H, Shames DM, Wendland M, et al. Correlation of dynamic contrast-enhanced MR imaging with histologic tumor grade: comparison of macromolecular and small-molecular contrast media. AJR Am J Roentgenol 1998;171:941–9.
4. Dvorak HF, Dvorak AM, Manseau EJ, Wiberg L, Churchill WH. Fibrin gel investment associated with line 1 and line 10 solid tumor growth, angiogenesis, and fibroplasia in guinea pigs. Role of cellular immunity, myofibroblasts, microvascular damage, and infarction in line 1 tumor regression. J Natl Cancer Inst 1979;62:1459–72.
5. Thurston G, Suri C, Smith K, et al. Leakage-resistant blood vessels in mice transgenically overexpressing angiopoietin-1. Science 1999;286:2511–4.
6. Thurston G, Rudge JS, Ioffe E, et al. Angiopoietin-1 protects the adult vasculature against plasma leakage. Nat Med 2000;6:460–3.
7. Stoeltzing O, Ahmad SA, Liu W, et al. Angiopoietin-1 inhibits vascular permeability, angiogenesis, and growth of hepatic colon cancer tumors. Cancer Res 2003;63:3370–7.
8. Gratton JP, Lin MI, Yu J, et al. Selective inhibition of tumor microvascular permeability by cavtratin blocks tumor progression in mice. Cancer Cell 2003;4:31–9.
9. Sima J, Zhang SX, Shao C, Fant J, Ma JX. The effect of angiostatin on vascular leakage and VEGF expression in rat retina. FEBS Lett 2004;564:19–23.
10. Satchi-Fainaro R, Mamluk R, Wang L, et al. Inhibition of vessel permeability by TNP-470 and its polymer conjugate, caplostatin. Cancer Cell 2005;7:251–61.
11. Goligorsky MS, Li H, Brodsky S, Chen J. Relationships between caveolae and eNOS: everything in proximity and the proximity of everything. Am J Physiol Renal Physiol 2002;283:F1–10.
12. Schubert W, Frank PG, Woodman SE, et al. Microvascular hyperpermeability in caveolin-1 (−/−) knock-out mice. Treatment with a specific nitric-oxide synthase inhibitor, L-NAME, restores normal microvas-

cular permeability in Cav-1 null mice. J Biol Chem 2002; 277:40091–8.
13. Drab M, Verkade P, Elger M, et al. Loss of caveolae, vascular dysfunction, and pulmonary defects in caveolin-1 gene-disrupted mice. Science 2001;293:2449–52.
14. Ackah E, Yu J, Zoellner S, et al. Akt1/protein kinase Bα is critical for ischemic and VEGF-mediated angiogenesis. J Clin Invest 2005;115:2119–27.
15. Dvorak HN, Senger DR, Dvorak AM, Harvey VS, McDonagh J. Regulation of extravascular coagulation by microvascular permeability. Science 1985;227:1059–61.
16. Dvorak HF, Nagy JA, Feng D, Brown LF, Dvorak AM. Vascular permeability factor/vascular endothelial growth factor and the significance of microvascular hyperpermeability in angiogenesis. Curr Top Microbiol Immunol 1999;237:97–132.
17. Gratton JP, Yu J, Griffith JW, et al. Cell-permeable peptides improve cellular uptake and therapeutic gene delivery of replication-deficient viruses in cells and *in vivo*. Nat Med 2003;9:357–62.
18. Razani B, Engelman JA, Wang XB, et al. Caveolin-1 null mice are viable but show evidence of hyperproliferative and vascular abnormalities. J Biol Chem 2001;276:38121–38.
19. Labrecque L, Royal I, Surprenant DS, Patterson C, Gingras D, Beliveau R. Regulation of vascular endothelial growth factor receptor-2 activity by caveolin-1 and plasma membrane cholesterol. Mol Biol Cell 2003;14: 334–47.
20. Lampugnani MG, Zanetti A, Corada M, et al. Contact inhibition of VEGF-induced proliferation requires vascular endothelial cadherin, β-catenin, and the phosphatase DEP-1/CD148. J Cell Biol 2003;161:793–804.
21. Tanimoto T, Jin ZG, Berk BC. Transactivation of vascular endothelial growth factor (VEGF) receptor Flk-1/KDR is involved in sphingosine 1-phosphate-stimulated phosphorylation of Akt and endothelial nitric-oxide synthase (eNOS). J Biol Chem 2002;277:42997–3001.
22. Zanetti A, Lampugnani MG, Balconi G, et al. Vascular endothelial growth factor induces SHC association with vascular endothelial cadherin: a potential feedback mechanism to control vascular endothelial growth factor receptor-2 signaling. Arterioscler Thromb Vasc Biol 2002;22:617–22.
23. Carmeliet P, Lampugnani MG, Moons L, et al. Targeted deficiency or cytosolic truncation of the VE-cadherin gene in mice impairs VEGF-mediated endothelial survival and angiogenesis. Cell 1999;98:147–57.
24. Zhao YY, Liu Y, Stan RV, et al. Defects in caveolin-1 cause dilated cardiomyopathy and pulmonary hypertension in knockout mice. Proc Natl Acad Sci U S A 2002;99:11375–80.
25. Garcia-Cardena G, Martasek P, Masters BS, et al. Dissecting the interaction between nitric oxide synthase (NOS) and caveolin. Functional significance of the NOS caveolin binding domain *in vivo*. J Biol Chem 1997;272: 25437–40.
26. Fukumura D, Gohongi T, Kadambi A, et al. Predominant role of endothelial nitric oxide synthase in vascular endothelial growth factor-induced angiogenesis and vascular permeability. Proc Natl Acad Sci U S A 2001;98:2604–9.
27. Murohara T, Asahara T, Silver M, et al. Nitric oxide synthase modulates angiogenesis in response to tissue ischemia. J Clin Invest 1998;101:2567–78.
28. Kashiwagi S, Izumi Y, Gohongi T, et al. NO mediates mural cell recruitment and vessel morphogenesis in murine melanomas and tissue-engineered blood vessels. J Clin Invest 2005;115:1816–27.
29. Liu J, Wang XB, Park DS, Lisanti MP. Caveolin-1 expression enhances endothelial capillary tubule formation. J Biol Chem 2002;277:10661–8.
30. Woodman SE, Ashton AW, Schubert W, et al. Caveolin-1 knockout mice show an impaired angiogenic response to exogenous stimuli. Am J Pathol 2003;162:2059–68.
31. Brouet A, DeWever J, Martinive P, et al. Antitumor effects of *in vivo* caveolin gene delivery are associated with the inhibition of the proangiogenic and vasodilatory effects of nitric oxide. FASEB J 2005;19:602–4.
32. O'Reilly MS, Boehm T, Shing Y, et al. Endostatin: an endogenous inhibitor of angiogenesis and tumor growth. Cell 1997;88:277–85.
33. O'Reilly MS, Holmgren L, Chen C, Folkman J. Angiostatin induces and sustains dormancy of human primary tumors in mice. Nat Med 1996;2:689–92.
34. Holmgren L, O'Reilly MS, Folkman J. Dormancy of micrometastases: balanced proliferation and apoptosis in the presence of angiogenesis suppression. Nat Med 1995;1:149–53.
35. Garcia-Barros M, Paris F, Cordon-Cardo C, et al. Tumor response to radiotherapy regulated by endothelial cell apoptosis. Science 2003;300:1155–9.
36. Ju H, Zou R, Venema VJ, Venema RC. Direct interaction of endothelial nitric-oxide synthase and caveolin-1 inhibits synthase activity. J Biol Chem 1997; 272:18522–5.
37. Bucci M, Gratton JP, Rudic RD, et al. *In vivo* delivery of the caveolin-1 scaffolding domain inhibits nitric oxide synthesis and reduces inflammation. Nat Med 2000;6: 1362–7.
38. Yoshiji H, Harris SR, Thorgeirsson UP. Vascular endothelial growth factor is essential for initial but not continued *in vivo* growth of human breast carcinoma cells. Cancer Res 1997;57:3924–8.
39. Shay-Salit A, Shushy M, Wolfovitz E, et al. VEGF receptor 2 and the adherens junction as a mechanical transducer in vascular endothelial cells. Proc Natl Acad Sci U S A 2002;99:9462–7.

Downloaded from http://aacrjournals.org/cancerres/article-pdf/67/6/2849/2580578/2849.pdf by guest on 06 November 2024